Proceedings of the ASME 2010 International Design Engineering Technical Conferences & Computers and Information in Engineering Conference
IDETC/CIE 2010
August 15-18, 2010, Montreal, Quebec, Canada

DETC2010-28814

SYMBOLIC MATH-BASED BATTERY MODELING FOR ELECTRIC VEHICLE SIMULATION

Aden N. Seaman
Department of Systems Design Engineering
University of Waterloo
Waterloo, Ontario, Canada. N2L 3G1
Email: anseaman@real.uwaterloo.ca

John McPhee
Department of Systems Design Engineering
University of Waterloo
Waterloo, Ontario, Canada. N2L 3G1
Email: mcphee@real.uwaterloo.ca

ABSTRACT

We present results of a math-based model of a battery electric vehicle (BEV) designed in MapleSim[1]*. This model has the benefits of being described in a physically consistent way using acausal system components. We used a battery model by Chen and Rinćon-Mora to develop a math-based model of a complete battery pack, and developed simple power controller, motor/generator, terrain, and drive-cycle models to test the vehicle under various conditions. The resulting differential equations are simplified symbolically and then simulated numerically to give results that are physically consistent and clearly show the tight coupling between the battery and longitudinal vehicle dynamics.*

1 Introduction

Vehicle modeling is a complicated and challenging task. Automotive companies release several new vehicles each year, and all of these need to be simulated and tested before they are actually manufactured.

With the push towards cleaner and more energy-efficient vehicles, powertrains are incorporating motors, generators, continuously-variable transmissions, energy storage devices such as batteries and fuel-cells, and traditional internal combustion engines (ICEs).

One of the techniques that can ease the growing complexity of vehicle modeling is acausal math-based modeling in which the system is described using the physics-based equations that govern the behaviour of its components. These mathematical equations are processed symbolically before finally being solved numerically to generate output data. This approach makes it easier for designers to specify component behaviour, and constrains them to describe components in a more physically-consistent language. This makes it easier to swap or modify components and simplifies the description of the system [1].

The Modelica [2] description language has been used by many authors [3–7] to model hybrid electric vehicle systems acausally, mostly using the Dymola [8] simulation environment.

We have chosen to use MapleSim [9] from MapleSoft as our simulation environment, as this allows us to access the underlying mathematical equations which govern the system being simulated.

This approach yields a simplified equation-based description of the system which can be simulated efficiently. The equations can also be used in real-time simulation for hardware-in-the-loop (HIL) applications, and can be used in sensitivity analysis and system optimization [10, 11].

In this paper we present the results of a battery electric vehicle (BEV) we have modeled using math-based modeling techniques in MapleSim. See Fig. 1 for a block diagram of the overall BEV system. This is the beginning of a more complex math-based hybrid electric vehicle (HEV) model we aim to develop using symbolic mathematics.

We have incorporated a lithium-ion electric-circuit battery model by Chen and Rinćon-Mora [12] into the BEV system. We

[1] Maple and MapleSim are trademarks of MapleSoft

modified the battery equations to simulate a battery pack composed of series and parallel combinations of single cells. In order to connect the battery pack to a motor we had to develop a power controller model as part of the system integration. We further incorporated a simple one-dimensional vehicle model that drives on an inclined plane, a terrain model that controls the incline, and a drive cycle model that controls the vehicle's desired speed.

By varying the drive cycle and terrain model, we tested the BEV under various driving conditions.

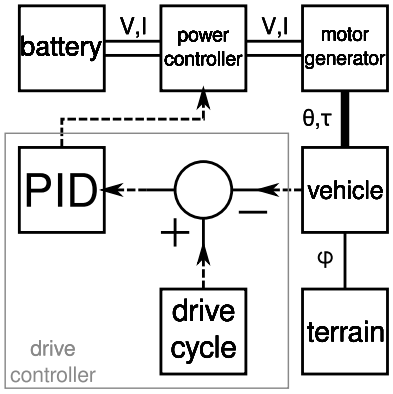

FIGURE 1. BLOCK DIAGRAM OF OVERALL BEV MODEL

2 System Modeling and Simulation

The technique we decided to use was math-based modeling using MapleSim as the simulation environment, which has a graphical interface for interconnecting system components. The system model is then processed by the Maple mathematics engine, and finally the differential-algebraic equations (DAEs) describing the system are simulated numerically to produce output data. For 3D multibody simulation it uses the DynaFlex-Pro engine, which uses linear graph-theory for system simulation [1, 11].

2.1 Battery

One of the most important components of an electric vehicle – either BEV or HEV – is the battery. There are many ways of modeling different battery chemistries depending on the fidelity needed and the battery parameters of interest. See the article by Rao *et al.* [13] for an overview of some of the techniques. Generally, with increasing model accuracy comes increased computational requirements.

Some modeling techniques that we reviewed were: the lead-acid model of Salameh *et al.* [14]; the mathematical lithium-ion model of Rong and Pedram [15] that incorporates state-of-health and temperature effects; the lumped-parameter model in section 3.1 of the Partnership for a New Generation of Vehicles (PNGV) Battery Test Manual [16]; the Kalman filtering techniques of Piller *et al.* [17]; the electrical circuit model of Chen and Rinćon-Mora [12]; and the impedance model of Nelson *et al.* [18]. These different techniques have their strengths and weaknesses and limited ranges of application.

There is a great interest in using lithium-ion batteries in electric vehicles, as they are light and have a higher power-to-weight and power-to-size ratio than Lead-Acid or Nickel-based batteries. Great demands are placed on vehicle batteries as the driver accelerates and brakes regeneratively, putting the batteries through periods of high current draw and recharge. Depending on the driving environment, the batteries can also be subjected to large temperature variations, which can have a significant effect on the battery's performance and lifetime.

Thus we needed to model a lithium-ion battery chemistry over a wide state-of-charge (SOC) range, under widely-varying currents, for various temperatures. Since we would eventually like to model this vehicle in a hardware-in-the-loop (HIL) system, we needed a model that was not computationally expensive, and we did not require a high-fidelity model.

These requirements led us to the electrical circuit model of Chen and Rinćon-Mora. We implemented their components in MapleSim and used a custom function block to represent the non-linear relationship between the state of charge and the electrical components (Equations 2 to 6 in their paper). See Fig. 2 for a block diagram of the battery.

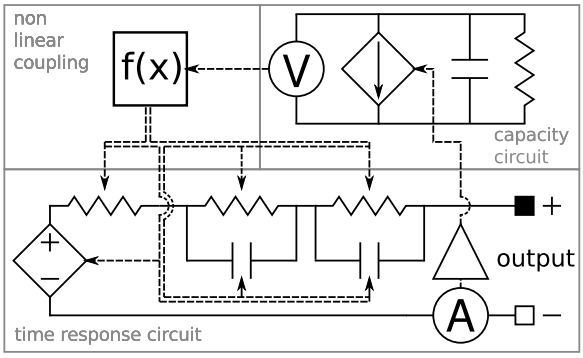

FIGURE 2. BLOCK DIAGRAM OF SINGLE-CELL BATTERY MODEL

Since their model is of a single cell, we modified their equations to simulate a battery of cells in parallel and series. The Chen and Rinćon-Mora battery can be divided into two linear circuits with a non-linear coupling between them. See Fig. 2 for labels of these different circuits. One circuit is a large capacitor in parallel with a resistor that models the charge state of the battery and self-discharge. This can be called the "capacity circuit". Another circuit is a voltage source in series with a resistor-

capacitor network that models the time response of the battery. This can be called the "time response circuit".

To adapt their single cell model to simulate an entire battery pack, let $N_{parallel}$ be the number of cells in a parallel pack, and let N_{series} be the number of parallel packs placed in series to make the whole battery. The open circuit voltage in the time response circuit is multiplied by N_{series}. The current flowing in the time response circuit is divided by $N_{parallel}$ when it flows in the capacity circuit. The resistors in the time response circuit are multiplied by $N_{series}/N_{parallel}$ and the capacitors are multiplied by $N_{parallel}/N_{series}$.

A single cell of the battery model has an open-circuit voltage of 3.3 V and a capacity of 837.5 mAh at a 1 A discharge rate starting at 100% state of charge. By placing 8 cells in parallel, and 74 of these parallel packs in series, a 244.2 V, 6.7 Ah battery pack was created. This pack is comparable to that in a 2007 Toyota Camry hybrid [19].

The Chen and Rinćon-Mora battery model is simple enough to simulate in a short amount of time while being complex enough to provide the following: variations in the open circuit voltage with SOC; transient effects of charge depletion and recovery and their dependence on SOC; and the variation in battery capacity with discharge current. Furthermore, since it is an electrical circuit model it can easily be incorporated into the electrical system of the BEV model and is amenable to being represented using math-based modeling techniques.

One of the downsides of this model is that no temperature effects of any kind are modeled, although Chen and Rinćon-Mora state it would not be difficult to include them. In an electric vehicle the temperature will vary with external environmental conditions, with heating of the battery due to internal losses, and with endo- and exothermic chemical reactions. The only model we encountered that explicitly included temperature dependence was the mathematical model of Rong and Pedram [15], but their model assumes a constant discharge current and thus is not suitable for our BEV system.

The Chen and Rinćon-Mora model can also be overcharged and does not consider the increasing resistance of the battery as it nears a full charge. Furthermore the variations of the battery's state-of-health (SOH) with time and charge cycles is not modeled. These downsides are acceptable given that in future modeling the vehicle's control system will limit maximum battery charge, and although in this paper we are not interested in modeling temperature or state-of-health, they should not be too difficult to incorporate.

2.2 Power Controller

The next important component of an electric vehicle is a power converter that acts as an interface between the battery and the drive motor/generator. This component controls the amount of power going to the motor during driving, and the amount of power going back into the battery during regenerative braking.

Generally, boost or buck converters are used depending on whether the output voltage is higher or lower, respectively, than the input voltage [20]. By varying the duty cycle of a high-frequency switching circuit, the output voltage and thus current and power can be controlled.

Instead of modeling the high frequency circuit in MapleSim, we decided to use a simple approximation that can serve as both a boost or buck converter with power flowing from the battery to the motor, or vice-versa. Figure 3 is a picture of the power controller block diagram. Although the current model has a fixed converter efficiency of 100%, a more realistic efficiency model such as the one used by Hellgren [3] can be incorporated.

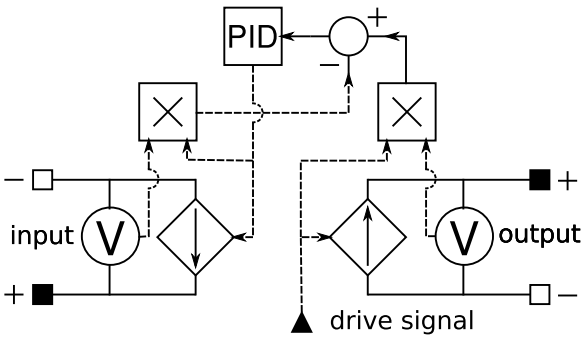

FIGURE 3. BLOCK DIAGRAM OF POWER CONTROLLER MODEL

Using a signal-driven current source in the output loop, the output voltage is measured and the output power is calculated. The input current is adjusted by a PID controller so that the input power matches the output power. This circuit works both for positive or negative current, which determines the direction of power flow. This model avoids the divide-by-zero problem of a simple algebraic power converter when the output voltage and current goes to zero, and adapts to changing input and output impedance. However it does not take into consideration physical limitations of components such as the battery's maximum charge or discharge rates, and voltage and current limits of the motor, wires, or power electronics.

2.3 Electrical Motor

The electrical motor used in the vehicle model is the Modelica DC permanent magnet motor, which includes internal resistance, inductance, and rotor inertia [21].

Its mechanical and electrical behaviour are modelled by Equations 1 and 2 where J_a is the armature inertia, $\theta(t)$ is the armature rotation angle, V_{nom}, I_{nom}, and f_{nom} are the nominal motor voltage, current, and rotational frequency, respectively. $\tau(t)$ is the shaft torque, and L_a and R_a are the armature inductance and

resistance, respectively. Finally $V(t)$, and $I(t)$ are the voltage and current at the motor terminals, respectively.

$$J_a\ddot{\theta}(t) - \frac{30(V_{nom} - R_a I_{nom})I(t)}{\pi f_{nom}} - \tau(t) = 0 \quad (1)$$

$$L_a\dot{I}(t) + R_a I(t) - V(t) + \frac{30(V_{nom} - R_a I_{nom})\dot{\theta}(t)}{\pi f_{nom}} = 0 \quad (2)$$

We chose to use the physical parameters of the LEM-200 Model D127 DC permanent magnet motor from L.M.C. Ltd [22]. However we modified the rated current and voltage of the motor to be more compatible with our battery voltage. This would effectively require re-winding the motor with different wire and changing its magnets.

The parameters used for the motor are presented in Table 1. Note that the peak current and power of the motor are twice the rated value.

TABLE 1. MOTOR MODEL PARAMETERS

Name	Value
Resistance	0.0175 Ω
Inductance	13 μH
Inertia	0.0236 kg · m^2
RPM_{rated}	3600 rpm
V_{rated}	150 V
I_{rated}	96 A
P_{rated}	12.56 kW

2.4 Vehicle Dynamics

The vehicle model we used was very simple. Its physical parameters were based on the 2007 Toyota Camry hybrid. Since we were concerned only with the performance of the powertrain components, we did not concern ourselves with vehicle suspension or steering. We used a one-dimensional model of a frictionless cart on an incline under the force of gravity. The drive motor is connected to one of the slipless wheels of the cart through a fixed transmission with a ratio of 9 motor revolutions per wheel revolution. The wheels have the same diameter as the P215/60VR16.0 tires on the Camry.

Equation 3 describes the relationship between the rotation and torque of the motor shaft. $\tau(t)$ is the torque seen at the motor shaft, m is the vehicle's mass, R is the drive tire radius, ρ is the gear ratio from the motor to the tire, $\theta(t)$ is the motor shaft's rotational displacement, g is the gravitational constant, and $\phi(t)$ is the terrain inclination angle.

Table 2 lists the values used for these parameters.

$$\tau(t) = \frac{mR}{\rho}\left[\frac{R}{\rho}\frac{d^2}{dt^2}\theta(t) + g\sin(\phi(t))\right] \quad (3)$$

TABLE 2. VEHICLE MODEL PARAMETERS

Name	Symbol	Value
mass	m	1613 kg
tire radius	R	32.25 cm
gear ratio	ρ	9
gravity	g	9.8 m/s^2

The only type of braking included in this model is regenerative braking where the current to the motor is reversed and the battery is charged with the kinetic energy of the vehicle. We did not take into consideration recharge current limits of the battery.

To this vehicle model we attached a simple terrain model. A time-dependent lookup table controlled the inclination of the terrain on which the vehicle traveled. This allowed us to simulate the vehicle's performance on flat and hilly terrain.

The drive cycle is a time-dependent lookup table of the vehicle's desired speed. A PID controller compares the desired speed to the actual speed and drives the input of the power controller to transfer power to the motor, or to extract power from the motor until the vehicle's speed matches the desired speed.

See Fig. 1 for the block diagram of the overall BEV model.

2.5 Numerical Simulation

After MapleSim converts the vehicle model into differential equations, it simplifies and reduces the system of equations symbolically. Then using this reduced equation set it solves them numerically to produce the final output data.

MapleSim simulated our system with its non-stiff solver, which uses a Fehlberg fourth-fifth order Runge-Kutta method

with degree four interpolant. We used an adaptive time-step with absolute and relative error tolerances of 1e-7, and turned on MapleSim's native code generation ability which runs the simulation faster. The model was simulated on a 3 GHz Intel Core 2 Duo using MapleSim version 3 for Linux. It was set to simulate over a 30 second time interval, and took 10 seconds of actual time to complete.

3 Results

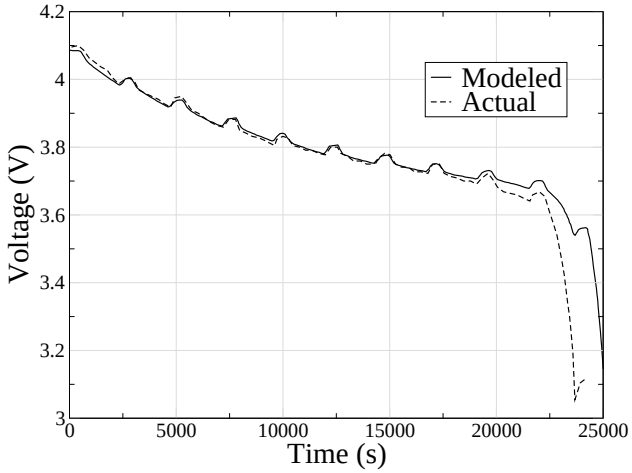

FIGURE 4. MODELED-VS-ACTUAL [12] BATTERY UNDER PULSED CONSTANT-CURRENT DISCHARGE

Figure 4 is a comparison between the MapleSim model and an actual cell for a pulsed current discharge of a single battery cell. The actual cell data was extracted from Fig. 5 of Chen and Rinćon-Mora's paper. Like the model in their paper, our model does not include a self-discharge resistor. An initial SOC of 98% gives a close match to the experimental results, tracking them very well until the battery capacity is almost exhausted. Our model requires one discharge cycle more than the actual to see a rapid collapse in the battery terminal voltage.

Using our vehicle model we performed two simple and intuitive tests. Table 3 lists the parameters used in the drive cycles.

3.1 Accelerations

The first test we did was to simulate the vehicle driving under hard and gentle accelerations on flat terrain. Battery and internal combustion engine vehicles are more efficient if gentle acceleration is used compared to hard acceleration, due to internal losses. The initial accelerations of the hard and gentle cycles are different, but the maximum speed and rate of deceleration are the same. See the hard and gentle curves of Fig. 5 for a plot of the drive cycle speed with time.

TABLE 3. DRIVE CYCLE AND TERRAIN MODEL PARAMETERS

Name	Value
V_{max}	9 m/s
a_{hard}	1.607 m/s^2
a_{gentle}	0.968 m/s^2
hill height	8.67 m
hill angle	8°

Figure 6 plots the battery's state of charge versus time. Recall that this model is without rolling resistance. One can see that the hard acceleration drive cycle ends up with a lower final state of charge than the gentle cycle. This difference is due to ohmic losses in the motor windings and chemical losses in the battery.

3.2 Hills

The second test we did was to drive the vehicle up and down a hill. The battery should lose energy going uphill as the vehicle gains gravitational potential energy, and gain energy going downhill as the vehicle loses potential energy. See the hill cycle curve of Fig. 5 for a plot of the drive cycle speed with time. The terrain cycle is very simple: at t=9.5 s the vehicle encounters the hill, then it drives up or down an 8° incline before returning to flat terrain at t=20.5 s.

Figure 7 plots the battery's state of charge versus time for this test. In both cases the battery loses energy as it accelerates

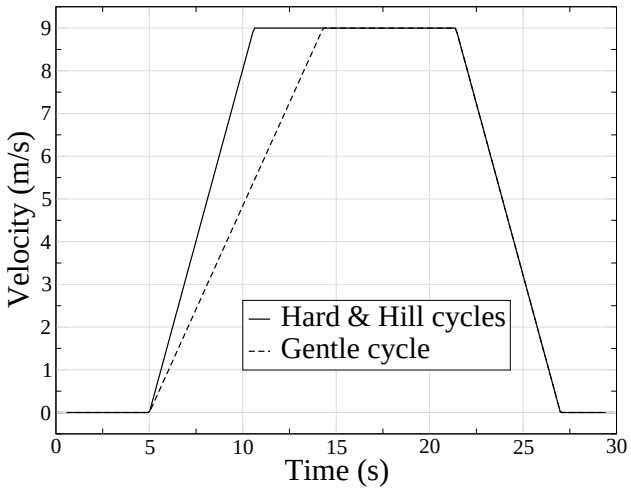

FIGURE 5. DRIVE CYCLE: SPEED-VS-TIME FOR HARD, GENTLE, AND HILL CYCLES

the vehicle, transferring energy from the battery to the vehicle's kinetic energy.

In the uphill case the state of charge decreases. The drive controller applies more power to the motor to match the vehicle's speed to the desired speed, and the battery's energy is put into the vehicle's gravitational potential energy.

In the downhill case the state of charge increases. The drive controller applies the regenerative "brakes" to keep the vehicle's speed constant, and the vehicle's gravitational potential energy is transferred to the battery.

Finally the vehicle encounters a flat spot and uses regenerative braking to come to a halt, transferring the vehicle's kinetic energy to the battery.

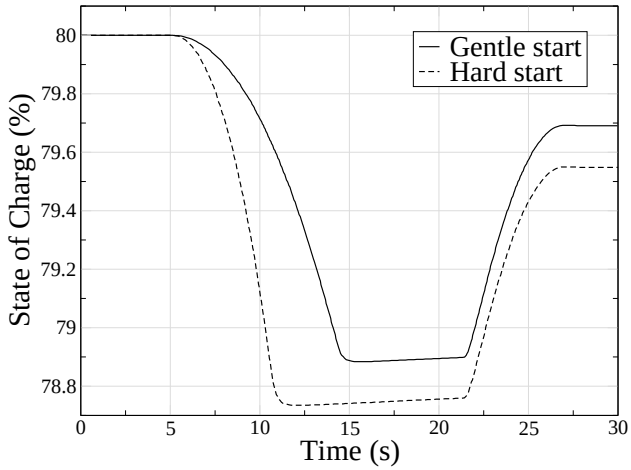

FIGURE 6. STATE OF CHARGE FOR HARD AND GENTLE ACCELERATIONS ON FLAT TERRAIN

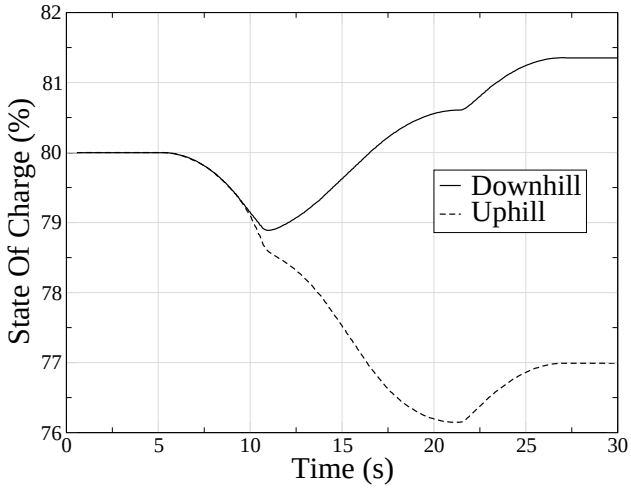

FIGURE 7. STATE OF CHARGE FOR UPHILL AND DOWNHILL CYCLES

3.3 Verification

A comparison can be made between the MapleSim results and approximate calculations based on energy conservation. The points of comparison on the hard and gentle acceleration cycles are before the vehicle starts moving, and after it has settled at its maximum speed, just before regenerative braking. Since the vehicle moves without rolling resistance on flat terrain, only the kinetic energy of the vehicle and the resistance losses in the motor and battery need to be considered.

See Table 4 for a comparison between the approximate theoretical calculations based on energy conservation and the MapleSim results for the hard and gentle acceleration cycles for the following quantities: J, the energy transferred into the vehicle; P, the average power during acceleration; ΔSOC, the change in the battery's state of charge taking into considering losses in the motor and battery. See Appendix A for the steps used in the hard drive cycle calculation.

TABLE 4. COMPARISON BETWEEN MAPLESIM AND APPROXIMATE THEORETICAL CALCULATIONS

Name	Approximate	MapleSim	% Difference
J_{hard}	65.326 kJ	66.64 kJ	2.01
P_{hard}	11.66 kW	11.9 kW	2.06
ΔSOC_{hard}	1.15%	1.2%	4.34
J_{gentle}	65.326 kJ	67.425 kJ	3.2
P_{gentle}	7.02 kW	7.25 kW	3.27
ΔSOC_{gentle}	1.055%	1.1%	4.265

The MapleSim results compare favourably with the approximate theoretical results. The small amount of difference is not surprising considering the simplicity of the approximate theoretical equations used.

4 Conclusion

We modeled a simple battery electric vehicle with math-based methods using MapleSim. This technique reduces development time and brings the system representation closer to the physics of the system.

Using a math-based model of a complete battery pack based on the battery model of Chen and Rinćon-Mora, a simple power controller model, and a standard Modelica DC motor we were able to put together a BEV powertrain and connect it to a simple vehicle dynamics model.

By applying different terrain conditions and driving cycles, two different scenarios were tested to compare the performance of our vehicle model to what one would expect from an actual vehicle. In both cases the results agreed with intuition and with approximate theoretical calculations.

The underlying mathematical equations describing the system can be used for sensitivity analysis, optimization, or for use in real-time HIL simulation.

Future work will include adding an internal combustion engine as a range-extender, increasing the fidelity of the power controller and motor model, and adding more complex vehicle, terrain, and drive cycle models to the system.

ACKNOWLEDGMENT

We would like to thank Toyota, MapleSoft, and the Natural Sciences and Engineering Research Council of Canada for funding and support.

REFERENCES

[1] Schmitke, C., Morency, K., and McPhee, J., 2008. "Using graph theory and symbolic computing to generate efficient models for multibody vehicle dynamics". *IMechE J. Multibody Dynamics,* ***222***, pp. 339–352.

[2] Modelica association. `http://www.modelica.org/`.

[3] Hellgren, J., 2002. "Modelling of hybrid electric vehicles in Modelica for virtual prototyping". In Proceedings of the 2nd International Modelica Conference, pp. 247–256. See also URL `http://www.modelica.org/events/Conference2002/papers/p32_Hellgren.pdf`.

[4] Laine, L., and Andreasson, J., 2003. "Modelling of generic hybrid electric vehicles". In Proceedings of the 3rd International Modelica Conference, pp. 87–94. See also URL `http://www.modelica.org/Conference2003/papers/h26_Laine.pdf`.

[5] Wallén, J., 2004. "Modelling of components for conventional car and hybrid electric vehicle in Modelica". MS Thesis, Linköpings universistet, May.

[6] Zhou, Y. L., 2005. "Modeling and simulation of hybrid electric vehicles". MS Thesis, University of Victoria.

[7] Simic, D., and Bäuml, T., 2008. "Implementation of hybrid electric vehicles using the VehicleInterfaces and the SmartElectricDrives libraries". In Proceedings of the 6th International Modelica Conference, pp. 557–563. See also URL `http://www.modelica.org/events/modelica2008/Proceedings/sessions/session5c.pdf`.

[8] Dymola: Multi-engineering and model simulation. `http://www.3ds.com/products/catia/portfolio/dymola`.

[9] Maplesim: High-performance multi-domain modeling and simulation. `http://www.maplesoft.com/products/maplesim/index.aspx`.

[10] Jalali, K., Uchida, T., McPhee, J., and Lambert, S., 2009. "Integrated stability control system for electric vehicles with in-wheel motors using soft computing techniques". *SAE Int. J. Passeng. Cars - Electron. Electr. Syst.,* ***2***, pp. 109–119.

[11] Vogt, H., Schmitke, C., Jalali, K., and McPhee, J., 2008. "Unified modelling and real-time simulation of an electric vehicle". *Int. J. Veh. Auto. Sys.,* ***6***, pp. 288–307.

[12] Chen, M., and Rinćon-Mora, G. A., 2006. "Accurate electrical battery model capable of predicting runtime and I-V performance". *IEEE Transactions on Energy Conversion,* ***21***(2), June, pp. 504–511.

[13] Rao, R., Vrudhula, S., and Rakhmatov, D. N., 2003. "Battery modeling for energy-aware system design". *Computer,* ***36***(12), December, pp. 77–87.

[14] Salameh, Z. M., Casacca, M. A., and Lynch, W. A., 1992. "A mathematical model for lead-acid batteries". *IEEE Trans. Energy Conv.,* ***7***(1), March, pp. 93–98.

[15] Rong, P., and Pedram, M., 2006. "An analytical model for predicting the remaining battery capacity for lithium-ion batteries". *IEEE Transactions on Very Large Scale Intergration (VLSI) Systems,* ***14***(5), May, pp. 441–451.

[16] US DEPARTMENT OF ENERGY, 2001. *PNGV Battery Test Manual,* 3rd ed., February. See also URL `http://avt.inel.gov/battery/pdf/pngv_manual_rev3b.pdf`.

[17] Piller, S., Perrin, M., and Jossen, A., 2001. "Methods for state-of-charge determination and their applications". *Journal of Power Sources,* ***96***, pp. 113–120.

[18] Nelson, P., Amine, K., Rousseau, A., and Yomoto, H., 2007. "Advanced lithium-ion batteries for plug-in hybrid electric vehicles". In Proceedings from the 23rd Electric Vehicle Symposium. See also URL `http://www.transportation.anl.gov/pdfs/HV/461.pdf`.

[19] U.S. D.O.E. advanced vehicle testing activity: 2007 Toyota Camry hybrid electric vehicle. `http://avt.inl.gov/pdf/hev/fact7129Camry07.pdf`.

[20] Bauman, J., 2008. "Advances in fuel cell vehicle design". PhD Thesis, University of Waterloo.

[21] Modelica standard library. `http://www.modelica.org/libraries/Modelica/`.

[22] L.M.C. Ltd. DC permanent magnet motor technical details, 200 table. `http://www.lmcltd.net/uploads/files/130_table.pdf`.

A Appendix A: Hard Driving Cycle Calculation

The average power, total energy, and change in state of charge will be compared between the MapleSim model and first principle calculations based on the conservation of energy. This is for the hard acceleration drive cycle conducted on flat terrain.

The maximum vehicle velocity is $V_{max} = 9\ m/s$ and the time during which it accelerates is $\Delta t = 5.6$ s, which is an acceleration of $a = 1.607\ m/s^2$. The vehicle mass is $m = 1613$ kg.

A.1 Powers and Energies

Theoretically, the total vehicle energy is $J = \frac{1}{2}mV_{max}^2 = 65.326$ kJ. The average power during acceleration is $P_{avg} = \frac{J}{\Delta t} = 11.66$ kW. Since the vehicle's velocity is linearly proportional to time, the vehicle's energy at any time can be written as $J(t) = \frac{1}{2}ma^2t^2$. The instantaneous power needed by the vehicle is then $P(t) = \frac{dJ(t)}{dt} = ma^2t$. Thus during the 5.6 seconds of acceleration, the required power is linearly proportional to time.

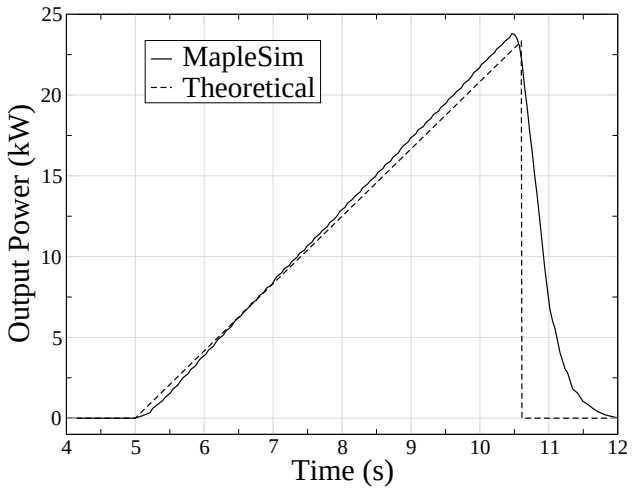

FIGURE 8. MAPLESIM AND THEORETICAL POWER TO MOTOR DURING HARD CYCLE ACCELERATION

See Fig. 8 for the theoretical and MapleSim's calculated power going into the motor during the hard cycle's acceleration period. In accordance with theory, the simulated power is seen to rise linearly with time over a period of 5.6 seconds up to a maximum value of 23.8 kW. The initial delay and final trailoff in the MapleSim results are due to the PID controller that is driving the vehicle. In MapleSim the average power is $P_{avg} = 23.8/2 = 11.9$ kW. The total energy can simply be calculated by the area under the triangle-shaped curve to give $J = 23.8 \times 5.6/2 = 66.64$ kJ.

These theoretical and simulated values appear in Table 4.

Here the battery losses do not need to be taken into consideration because the theoretical and MapleSim results are based only on the energy going into the motor. The MapleSim results do include losses due to the resistance of the motor armature which the theoretical results do not incorporate, but these losses are negligibly small as will be demonstrated in the next section.

A.2 State of Charge

The state of charge calculation is significantly more complicated, as the battery losses need to be taken into consideration. The time response circuit of the Chen and Rinćon-Mora battery model contains a resistor, and two parallel resistor-capacitor circuits in series. It will be shown that during the period of acceleration the resistances of the resistor-capacitor circuits can be neglected.

The current flowing through a parallel resistor-capacitor circuit is related to the voltage across them by the following equation:

$$C\frac{dV(t)}{dt} + \frac{V(t)}{R} = I(t) \tag{4}$$

The power flowing out of the battery is expressed by $P(t) = V(t)I(t)$. If we assume that the battery terminal voltage is constant, then $I(t) = P(t)/V = ma^2t/V = At$ where A is a constant and the current is linearly proportional to time.

Substituting this into Equation 4 and solving for $V(t)$ with the initial condition $V(0) = 0$ yields

$$V(t) = RA\left[t + RC\left(e^{\frac{-t}{RC}} - 1\right)\right] \tag{5}$$

Now to find the equivalent resistance of the circuit at any time we need to evaluate $R_{eq}(t) = \frac{dV(t)}{dI(t)}$. Since $I(t) = At$ then $dI(t) = Adt$. Implicitly differentiating Equation 5 with respect to time, collecting the Adt term, then dividing both sides by Adt gives:

$$R_{eq}(t) = \frac{dV}{dI} = \frac{dV}{Adt} = R\left(1 - e^{\frac{-t}{RC}}\right) \tag{6}$$

At $t = 0$ the equivalent resistance of the parallel circuit is zero. As $t \to \infty$ the equivalent resistance approaches the value of the resistor, R.

Thus the equivalent resistance depends on the time over which the current flows through the circuit. The time constant of the circuit is simply RC. For our battery pack of 8 parallel

cells and 74 packs in series at 80% state of charge the time constants for the short time response, and long time response circuits are 32.85 s and 223.03 s, respectively.

Since the vehicle only accelerates for 5.6 seconds, both of these time constants are significantly larger than the acceleration time, and thus the resistance of both parallel circuits can be ignored in favour of the battery's series resistance, which is $R_{series} = 0.668\,\Omega$. When analysing the voltage-vs-current behaviour of the battery using MapleSim, this conclusion is justified.

So instead of being constant, a better approximation of the battery's terminal voltage is $V(t) = V_{oc} - R_{series} I(t)$, and the relationship between power and current is $P(t) = ma^2 t = [V_{oc} - R_{series} I(t)] I(t)$. Solving this equation for $I(t)$ gives:

$$I(t) = \frac{V_{oc}}{2R_{series}} - \frac{1}{2}\sqrt{\frac{V_{oc}^2}{R_{series}^2} - \frac{4ma^2 t}{R_{series}}} \tag{7}$$

The negative root is taken since $I(0) = 0$. Substituting in the numerical parameters of the model gives us $I(t) = 210.756 - 77.781\sqrt{7.336 - t}$ for t = 0 to 5.6 s.

The power losses due to the various resistors are $P_{losses}(t) = I(t)^2 [R_{series} + R_{motor}]$. The energy losses can be calculated as:

$$\begin{aligned} J_{losses} &= J_{\underset{battery}{loss}} + J_{\underset{motor}{loss}} = \int_0^{5.6} P_{losses}(t)\,dt \\ &= [R_{series} + R_{motor}] \int_0^{5.6} I(t)^2\,dt \end{aligned} \tag{8}$$

This yields $J_{\underset{battery}{loss}} = 12.45$ kJ and $J_{\underset{motor}{loss}} = 0.30$ kJ. One can see that the motor losses are 41.5 times smaller than the battery losses, and over 200 times smaller than the overall vehicle energy. This is why they can be ignored in the calculation of powers and energies.

Now the battery's starting energy can be calculated based on the capacity, terminal voltage, and an hour-long 1C discharge using the equation $J_{battery} = 6.5\text{ Ah} \times 290\text{ V} \times 3600\text{ s/h} = 6786$ kJ.

The total energy spent by the battery in accelerating the vehicle is $J_{output} = J_{vehicle} + J_{losses} = 65.326 + 12.754$ kJ. The percentage of the total battery energy that this represents yields the change in the state of charge $\Delta SOC = J_{output}/J_{battery} \times 100\% = 78.08/6786 \times 100\% = 1.15\%$. This is the value that appears in Table 4.